Carbon Nanotube Dry Spinnable Sheets for Solar Selective Coatings by Lamination

Patricia M. Martinez[1], Vladimir A. Pozdin[2], Alexios Papadimitratos[2], William Holmes[2], Fatemeh Hassanipour[1], George Dover[3] and Anvar A. Zakhidov[1,2,4,5*]

[1]NanoTech Institute, University of Texas at Dallas, Richardson, TX 75083–0688, USA
[2]Solarno Inc., Irving, TX 75061, USA
[3]Department of Physics and Astronomy, University of Surrey, Guildford, GU2 7XH, UK
[4]National University of Science and Technology, MISiS, 119049, Leninskiy prospekt 4, Moscow, Russia
[5]ITMO University, 191002, Lomonosova street, 9, St. Petersburg, Russia

Article info

Received:
20 February 2016

Received and revised form:
15 April 2016

Accepted:
18 June 2016

Abstract

Carbon nanotube, oriented free standing sheets can be laminated on any surface as selective solar absorbers while simultaneously dry spun in a highly controlled process from vertically oriented forests grown by CVD. We have found that properties of a CNT forest strongly correlate with the optical transparency and reflectivity of CNT sheets required for solar selective coatings and can be properly tuned for optimal coatings for solar collectors. We study absorptive and emissive properties of CNT sheets that are laminated by a simple automated and controlled process, developed for coating of cylindrical glass tubes for evacuated solar collectors (ETC). The advantages of Joule heating of CNT coatings are demonstrated and test results described, showing a unique property of fast heating as compared to slow heating in conventional solar water heaters.

1. Introduction

In Solar energy systems, the power of light is usually converted into electrical energy via photovoltaic technology or transformed directly into thermal energy by utilizing solar thermal collectors, specifically solar water heaters (SWH). The most recent report claimed that 35% of the global energy consumption in residential and industrial sectors was designated for lighting, water heating and electrical devices. Among these, domestic water heating accounted for 30% of the total energy consumption. The introduction of SWH systems to improve upon non-renewable energy sources has been highly profitable, efficient and, as a zero CO_2 emission technology, does not contribute to global warming [1–3].

In a SWH system, incident solar energy is converted to heat by a solar collector, transferred through a transfer medium, such as water, and finally moved to a hot water storage tank. The most important part of a SWH is the solar collector. It is the active part that converts the incident solar radiation into heat [4–6].

Solar collectors are classified as non-concentrating or concentrating depending on how they harvest the solar energy [7]. Non-concentrating systems have a collector area that intercepts the solar energy which is the same size as the absorber area that absorbs the solar energy. These systems are intended to produce domestic hot water at temperatures around 60 °C. Concentrating collectors use various reflectors, mirrors and concentrators to focus the solar energy onto a small area which can produce temperatures around 400–1000 °C. Their use is strictly industrial and they are mainly found in power plants [7].

Among the non-concentrating systems two different types of solar collectors are prominently used: flat plate and evacuated tubes. Flat plate collectors consist of an absorber plate with fluid tubes running through it, an insulation material to reduce heat losses, and a cover glass top to reduce radiation back to the atmosphere [8–10]. The absorber plate is a thin sheet of steel, copper or a thermal stable polymer with a flat, corrugated or grooved plate morphology covered with a solar selective coating.

*Corresponding author. E-mail: zakhidov@utdallas.edu

The coating is normally black to maximize the absorption for shortwave solar energy while losing as little heat as possible [11]. The top cover is glazed with multiple layers of glass or other materials with a transmissivity preference for short wave radiation and a blockage for long wave radiation [6].

Evacuated tube collectors consist of two concentric glass tubes fused at one end and sealed under vacuum to minimize heat loss [12]. The inner tube is coated with a black solar absorbing material. The heat converted by the solar collector is extracted from the evacuated system using a heat pipe, a u-tube pipe or by direct water flow [7].

An efficient way to increase the solar collection efficiency of a SWH is to apply an efficient selective solar absorber coating to the collector. An ideal solar absorber has zero reflectance in the visible region, high reflectance in the infrared region and low thermal emittance [7]. Black coatings are widely used as absorber coatings in SWH due to their high solar absorbance even though they poses high thermal emissivity [13]. Metals by themselves present high reflectance and suppression of thermal emittance in the high infrared region; however, they lack in solar absorbance. Good conductors and reflectors such as Au, Ag, Al and Cu present thermal emittances of 0.01–0.04 up to temperatures of 300 °C, but their solar absorption is poor [14]. Semiconductors and transition metals have been proven to be sufficient single element solar absorber candidates, but their compositions are required to be greatly modified [7]. Solar absorber coatings often combine different materials in order to achieve the required requisites. For example, Al_2O_3/Mo/ Al_2O_3 [15], Cr-Cr_2O_3 [13] and SS-AIN [16] have been successfully used, but require the use of expensive and complicated deposition methods [7].

Other materials such as carbon nanotubes have been reported to be nearly–perfect optical absorbers with theoretical ultra-low reflectance within the range of 0.01–0.10% in the visible region [17]. According to Yang et al., the key for an ultra-low reflectance is the introduction of long, low-density and well-aligned nanostructures which, when assembled in an aligned manner, have deep apertures [18]. They were able to obtain a total reflectance of 0.045% by using multiwall carbon nanotube (MWNT) forest with heights between 10–800 μm and densities between 10–20 μg/cm. To our knowledge, the use of MWNT forest as solar absorbers in SWH have yet to be successfully implemented. Size limitation of CVD chambers and the delicateness of the MWNT forest has not made it possible to exploit this technology as solar absorbers. However, the use of carbon nanotube ink solutions as solar absorbers has been explored. Chen et al. prepared a solar absorber with absorption of 90% and thermal emissivity of 0.13 using electrophoretically deposited aligned carbon nanotubes on top of aluminum substrates [19]. According to their results, a high solar absorption and low reflectance in the visible spectrum, as well as high reflectance in the infrared region is found in ticker carbon nanotube coatings. Nevertheless, the thermal emissivity increases as the film thickness increases [20]. Carbon nanotube ink solutions may not be a scalable and commercial technology as a coating for solar collectors because it requires the immersion of the entire material into the solution and would be difficult to apply precisely to specific areas.

Well-aligned sheets spun from vertically aligned MWNT forest, that can be spanned into transparent MWCNT sheets [2–4, 21], have not been yet investigated as solar absorber coatings before, although many other applications has been suggested for transparent thin CNT sheets, such as transparent electrodes for solar cells [5], and for OLEDs [6], and also as cold electron emitters for various type displays [7, 8].

2. Experimental

2.1. CNT synthesis

Carbon nanotube coating was prepared by pulling sheets from vertically aligned forests. Carbon nanotube forests were grown using chemical vapor deposition [22]. Silicon wafers with a 100 nm layer of silicon dioxide were used as substrates. First, a thin layer of iron catalyst film was deposited on top of the substrates using electron beam deposition to achieve a thickness of 3–5 nm at a rate of 0.1 Å/s. Then, substrates were cut into 3 by 4 cm pieces that were loaded into the quartz reaction chamber on a quartz boat. The diameter of the quartz chamber used for synthesis was 7.5 cm. The reaction chamber was evacuated and sustained under helium flow of 2400 sccm during the temperature ramp. The target temperatures of the three zone furnace were 840 °C and 725 °C for the pre-heat and post-heat zones respectively, with the central reaction zone varying in temperature between 700–750 °C. The ramp time was 20 min. The synthesis began when the mixture of acetylene at 116.8 sccm and hydrogen at 1354 sccm was allowed to enter the reaction chamber. The actual synthesis time was varied to produce forests of various heights. Upon completion of the synthesis, reaction gasses were turned off and the system was allowed to cool to room temperature under helium flow of 1200 sccm.

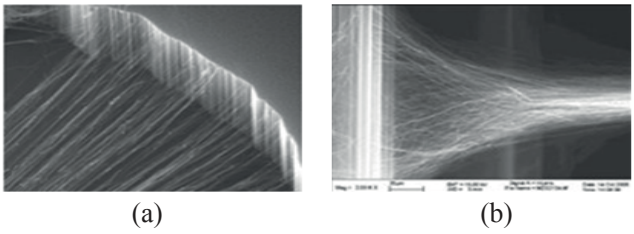

(a) (b)

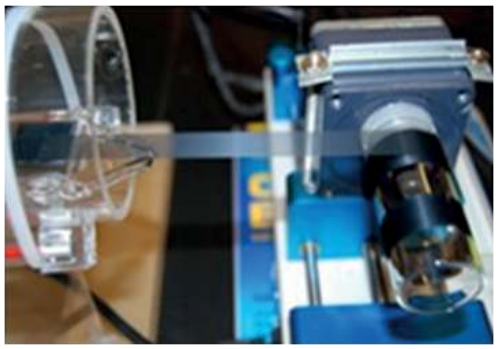

(c)

Fig. 1. The dry drawing of carbon nanotube (CNT) sheets: (a) from CVD grown CNT forest; (b) sheet being drawn from vertical forest; (c) motorized setup of CNT-sheet drawing of CNT forest followed by lamination on glass cylinder of ETC.

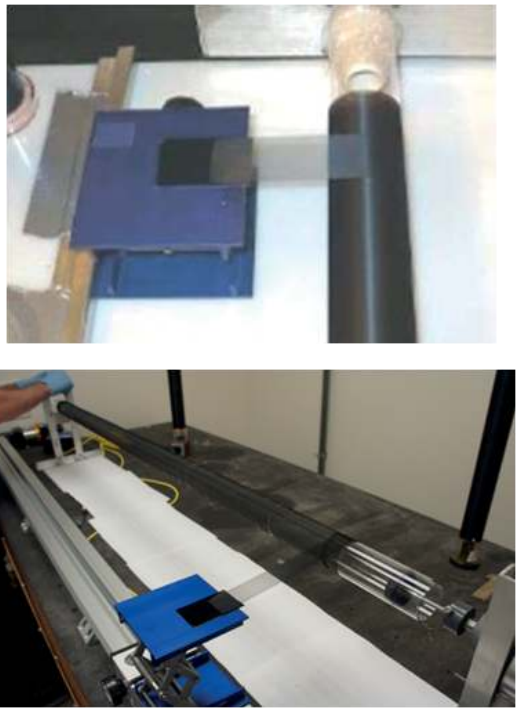

Fig. 2. (a) Automated lamination process to coat tubular solar collectors with solar selective coatings of MWNT; (b) Computer controlled continuous lamination system developed by Solarno for dry lamination of CNT sheets on inner tube of ETC selective solar collector.

CNT coating exhibit properties dependent on the height of the forest from which it is spun. The performance of SSC made with CNT from forest with various heights is shown in Fig. 1b. Once again, there was no significant difference in the heating rates between the different coatings. CNT coating created with a 340 μm forest exhibited the highest temperature increase, while the 100 μm forest resulted in the smallest temperature increase. The coating from the tallest forest (520 μm) was the second best performing. Aliev et al. (2009) predicted that short forests result in lower thermal conductivity than tall forest due to increased bundling between nanotubes per unit length of spun sheet, which suppresses phonon modes and decreases thermal transport [23]. This trend was observed for CNT solar absorbers made from all, but the tallest forest. This warranted a detailed investigation on how the height of the CNT forests affects the thermal transport of the solar absorbers.

CNT forests were grown for 10 min at 700–750 °C while maintaining all other growth parameters constant. Forest height increased from 100 to 520 μm as the temperature increased from 700 to 750 °C, respectively. Since the probability of defects occurring in the nanotubes increases with increasing forest synthesis temperature, taller forests are expected to have more intrinsic defects than shorter forest [24–27]. Therefore, the low thermal transport of the tall 520 μm forest can be explained by looking at its morphology, Fig. 2. SEM imaging of this forest revealed a wavy-like CNT forest with ~ 50 nm bundles which is characteristic of tubes grown at long synthesis times [26]. Sheets pulled from the side of this forest align along the tube direction with thicker bundles and maintain the forest's intrinsic waviness.

2.2. Sheet pulling on small and large scale

In Fig. 2 a-b, the lamination system for coating CNT sheets at large scale is shown. The inner tube of an evacuated solar collector was mounted on table and it was rotated with the help of a motor. The CNT aerogels sheets, used to fabricate the solar absorbing coating, were coated on the inner tube and pulled from the CNT forest. The CNT forest is placed on a moving stage in order to coat the entire surface of the tube. Once the initial sheet is pulled, the CNT forest stage begins to move while the tube rotates. The lamination system allows great control and morphology of the laminated CNT layer and can be used to coat full size solar evacuated collectors (180 cm). The current average time to fabricate a prototype CNT coated solar collectors was 45 min. The coating can be easily accelerated by increasing either the speeds of stage or rotating motor or the size of forests.

2.3. UV-Vis measurements

Optical transmittance and reflectivity of carbon nanotube sheets were investigated using Perkin Elmer Lambda 900 UV-Vis/NIR Spectrophotometer. Integrated sphere attachment was used for reflectivity measurements. Commercial solar collectors obtained for comparative measurements were Apricus Al-N-Cu/Al and WesTech TiNOx.

2.4. Emissivity measurements

Thermal emissivity of the samples, ε_{th}, at 100 °C was measured using an FTIR E40 infrared camera. A heat gun was used to heat the samples to 100 °C with a thermocouple attached to monitored the surface temperature. The emissivity was obtained by matching the actual sample surface temperature to the reading on the FTIR camera.

2.5. Testing in HV system

In order to simulate the conditions of a completed solar collectors, where the SSC is located in vacuum between two concentric glass tubes, miniature solar collectors (15 × 15 cm) were prepared and evaluated inside a custom vacuum chamber at high vacuum (10^{-5} Torr). Perkin Elmer solar simulator source calibrated to AM 1.5 was used to illuminate a section of the solar selective coating. Surface thermocouples were mounted inside the miniature collector in two locations: one on the illuminate section and another on the opposite and non-illuminated section. Under illumination, thermocouple logger recorded the temperature increase due to absorption and transmission of the solar energy.

2.6. Joule heating

The CNT coating collector was used to evaluate the performance of joule heating. To eliminate the effect of the heat pipe on the performance, the inside of the collector was directly filled with 1000 ml of water. Using the specific heat of water and the known applied power to the carbon nanotube coating ($P = V \times I$), it is possible to calculate the efficiency of the Joule heating, as $\eta_{joule} = \frac{cm\Delta T}{VIt}$, where t is time.

3. Results and discussion

3.1. Optical Properties

Figure 3a shows the results of UV-Vis measurements on carbon nanotube sheets of various thickness. The absorption of carbon nanotubes is an additive property, which is to say that it depends on the number of sheets stacked on top of each other. As the number of sheets increases the transmission decreases. Carbon nanotube sheets exhibit very low reflection and just 5 undensified layers achieved <3% reflectance over the solar spectrum, see Fig. 3a. Further addition of layers reduced the reflection marginally, and beyond 10 layers the reduction in reflection was not justified by the added material. At the same time, the transmission of 5 undensified layers of carbon nanotubes is high in the solar spectrum and additional layers were needed to approach the saturation value. Densification significantly decreased the transmission of carbon nanotube sheets and marginally increased the reflection. Nevertheless, the overall effect of densification was the increase in the absorption of carbon nanotube sheets. The increase in reflection upon densification is attributed to the reduction of scattering centers as the collapsed CNT aerogel network. Based on these results, 10-layer carbon nanotube coating was sufficient for absorption of most of the solar spectrum and further investigation of carbon nanotube sheet properties focused on 10 layer thick samples. It is important to point out that these results are characteristic of carbon nanotubes grown under the described conditions and variation in growth parameters will lead to some variations in observed properties.

The solar selective coating is typically partially transparent, but the structure of the solar collector traps any transmitted light by reflection from a metal base coating and reabsorption or, in the absence of a metal base coating, the absorption by the backside selective coating. For this reason, the reflection is one of the two most important metrics of a solar selective coating. Figure 3a, shows the reflectance of the carbon nanotube sheet coatings and of the commercially available coatings. Carbon nanotube coatings outperform the commercial coating with reflection of 2% and 4% for undensified and densified coatings, respectively. By comparison, best performing commercial coating reflected nearly 9% with large losses in the high-energy, low-wavelength part of the spectrum. Carbon nanotube coating showed great potential for solar selective coating due to the extremely low reflectance, even in the UV region, which is important for the harvesting of solar energy on an overcast day.

From the optical data, the difference between densified and non-densified carbon nanotube sheet coatings is clear, but the performance as solar selective coating is convoluted. Solar selective coating must have not only good absorption and low reflec-

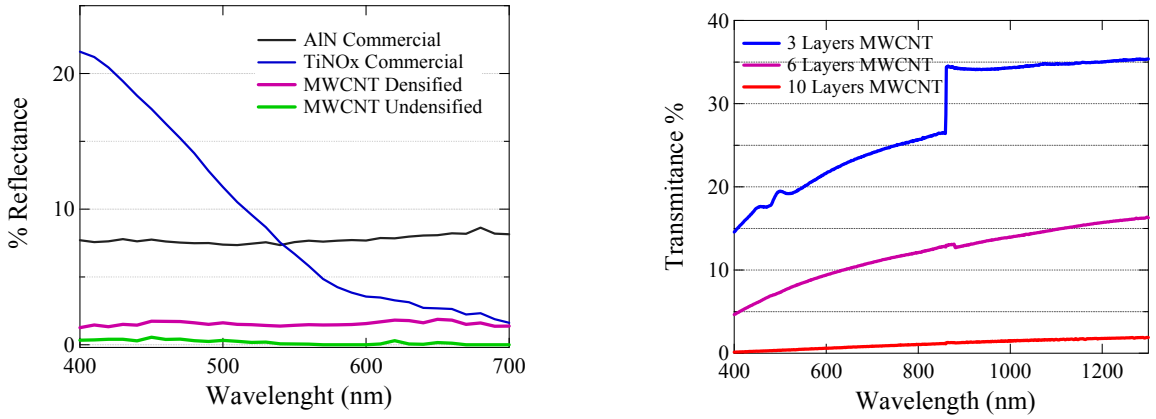

Fig. 3.(a) Reflectance and (b) Transmittance of densified CNT sheets of varying thickness. Densified sheets result in slightly increased reflectance as compared to undensified sheets, but this is offset by the significant increase in absorption of densified sheets. Approximately 10 layers of densified CNTs are sufficient to achieve high absorption.

tion, but also good thermal conductivity, low thermal resistance between the glass and the coating, and low emissivity. In order to test the performance of carbon nanotube sheet selective coating, prototype collectors were created on the base of small glass test tubes.

Densified carbon nanotube sheets exhibited higher final temperature inside the glass tube, as compared to non-densified, see Fig. 4. This difference cannot be explained by optical properties along, because densified carbon nanotubes have slightly higher reflectivity than non-densified and therein the amount of energy absorbed by the densified carbon nanotube coating is less. Improved thermal conductivity of densified sheets or reduced thermal contact between the CNT coating sheet and glass would manifest as increased heating rate of the coating, but no significant difference has been observed between densified and undensified sheets. Therefore some other property variation, such as emissivity plays a big role in the performance of CNT solar selective coating to make up this difference in performance. In fact, the measured emissivity of non-densified carbon nanotube sheets is ~0.98, while densified sheets have emissivity of 0.7.

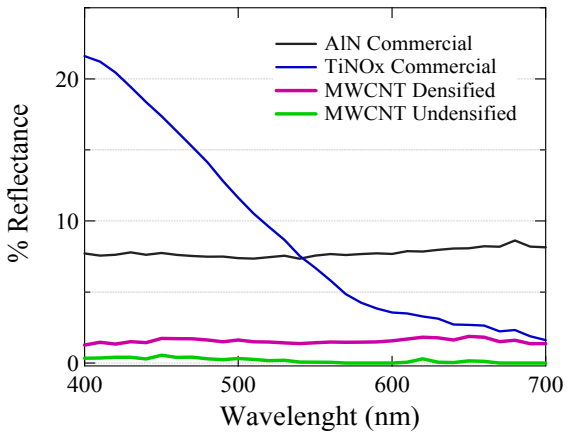

Fig. 4. The comparison of reflection between CNT coatings and commercially available solar selective coatings such as TiNOx and AlN.

Based on the heating rate and the ΔT achieved we evaluated the performance of the solar selective coating. First priority was to determine the optimal forest height for the solar selective coating; forests of various heights were tested and it was determined that forest height of approximately 350 μm was the best, see Fig. 5. There is not significant different in the heating rates of the various forests, but the final temperature and the ΔT are significantly different. Carbon nanotube coating created with 340 μm forest exhibited the highest temperature increase, while the 100 μm forest resulted to the smallest temperature increase.

It was surprising that the tallest forest (550 μm) did not exhibit the best performance as has been theoretically predicted [28]. This discrepancy was attributed to the reduced properties of the taller forests, wherein forest's vertical growth rate decreases and carbon nanotubes start bending and growing laterally. A pulled sheet of poorly aligned or bent nanotubes produces reduced overlap between carbon nanotubes and increases scattering. These effects reduce the thermal conductivity leading to reduced ΔT and any increases in light scattering are negligible, because carbon nanotubes reflection is low (<2%) even in short forests.

It is well known that MWNT growth is reaction temperature and time dependent. When the reaction temperatures and times are increased, specifically at temperatures greater than 780 C and reaction times greater than 20 min, defects caused by catalyst deactivation and the formation of amorphous carbon

decreases the forest spinnability. By changing the reaction temperature from 700 to 750 °C and keeping all other parameters constant, we observed the resulting forests' heights increased from 150 to 400 µm. As consequence, at temperatures greater than 800 C the spinnability of the forest decreased and forest imperfection start to appear.

When the reaction time is increased from 4 to 10 min using the same growth parameters, the height is increased from 150–400 µm. In this case the spinnability and density are increased. Therefore, in order to get spinnable forest in the range of 400–550 nm a right combination of time and temperature were adjusted.

Figure 6 shows the morphology of the tallest forest tried as a solar coating. The presented waviness is characteristic of a forest grew at longer reaction times and correspond to regions with high intrinsic concentration of defects of individual MWNT [29, 30].

Taking into consideration that taller MWNT forest have in general more intrinsic defect, it is now clear the sheets coming from this type of forest and used as solar coatings will not perform as well as sheets coming from medium length MWNT forest with less defects. The intrinsic defects in the MWNTs will create a higher phonon scattering when heated leading to a reduction in the thermal conductivity that can be reflected as a lower maximum achieved temperature [28].

In order to test the Joule heating capability of carbon nanotube selective coating, we created a CNT coated collector with electrical connections to the selective coating. Two contacts have been added to allow current to be applied across the conductive CNT coating. The collector was filled with 700 ml of water. Stirring rod was used to agitate the water and ensure accurate thermocouple readings, as Joule heated coating creates a significant temperature gradient across non-perturbed water.

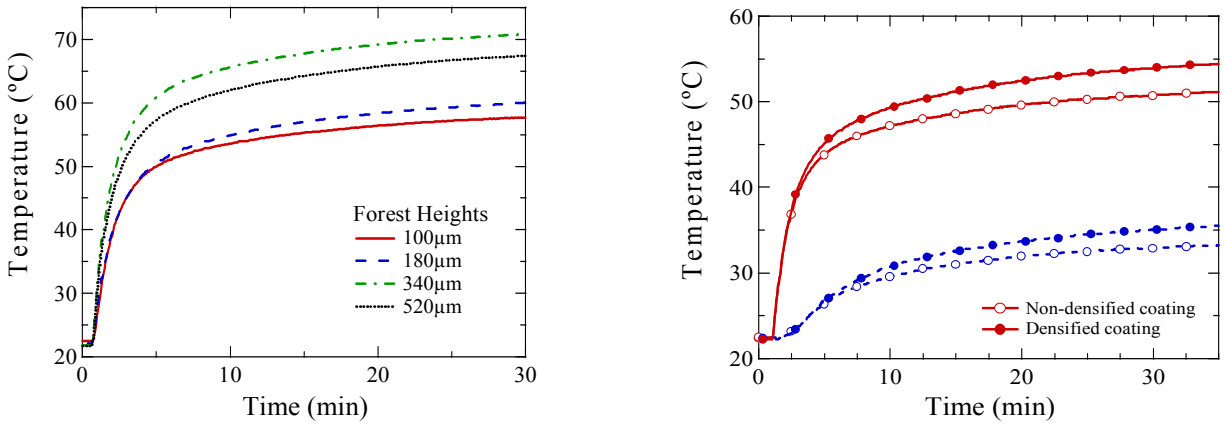

Fig. 5. (a) Measurements of prototype carbon nanotube coatings based on forests with various heights. (b) Temperature of the inner part of the glass tube coating with carbon nanotube sheets under AM 1.5 illumination. After non-densified coating was measure, it was densified with IPA and measured again.

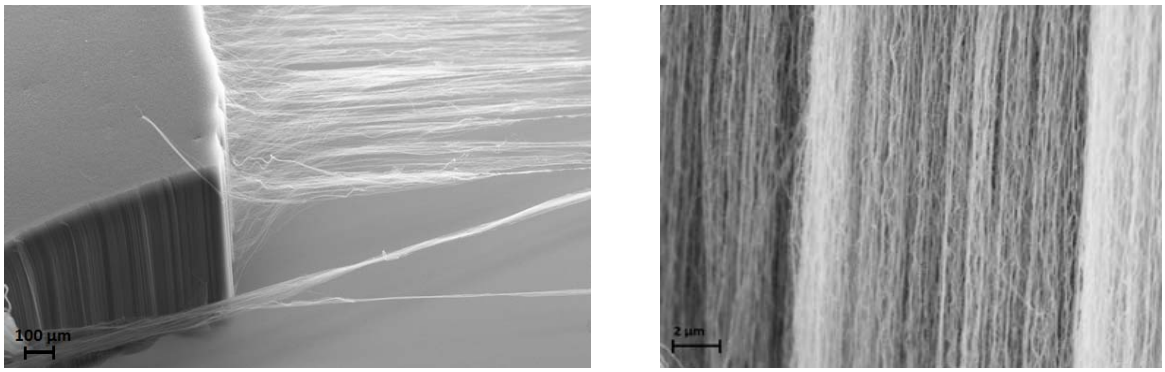

Fig. 6. SEM images of 550 µm tall carbon nanotube forest grown at Si coated by Fe catalyst showing the characteristic waviness of MWNT grown at higher temperature and reaction time.

As shown in Fig. 7, the water inside the collectors reaches temperature of over 90 °C in less than 180 min with the application of 37 Watts on average. The efficiency of such heating starts at 90% and slowly decreases with increasing temperature due to thermal losses to the ambient environment.

Figure 8 shows the testing of tube with joule heating effect. The current caused the CNT coating to warm up and therefore heat the water inside the tube. The power source was a typical outlet 110 V. The temperature of water was recorded.

In the case of joule heating tube, it was tested inside the lab and the increase of water was significantly accelerated. To achieve the increased temperature, we recorded only 47 W and 0.05 kWh.

The water heating rate shown in Figs. 8 and 9 is impressive in comparison with the heating rate of commercial solar collector, which is capable of heating water from 20 °C to only 55 °C on a sunny Dallas day over the course of 3 h. As measured previously, the emissivity of the carbon nanotube coating is 0.7, which constitute large energy losses with increasing temperature; a number of pathways are being pursued to significantly reduce the emissivity below 0.1, similarly to the commercial coatings. With reduced emissivity and optimized power output, the efficiency can be further improved in the future. For an early stage prototype, this result is very promising.

Slow heating and the necessity for solar energy are major drawbacks of solar water heaters. In the real world, solar water heater systems are unable to generate hot water until late morning, which is after the morning peak consumption. Therefore, the systems rely on booster hardware and the unspent reserves from the previous night. Utilizing Joule heating capability of the carbon nanotube coated evacuated tube collector would remove the need for booster hardware and through the use of a feedback system allow the solar water heater operate at the optimal temperature achieve the highest efficiency.

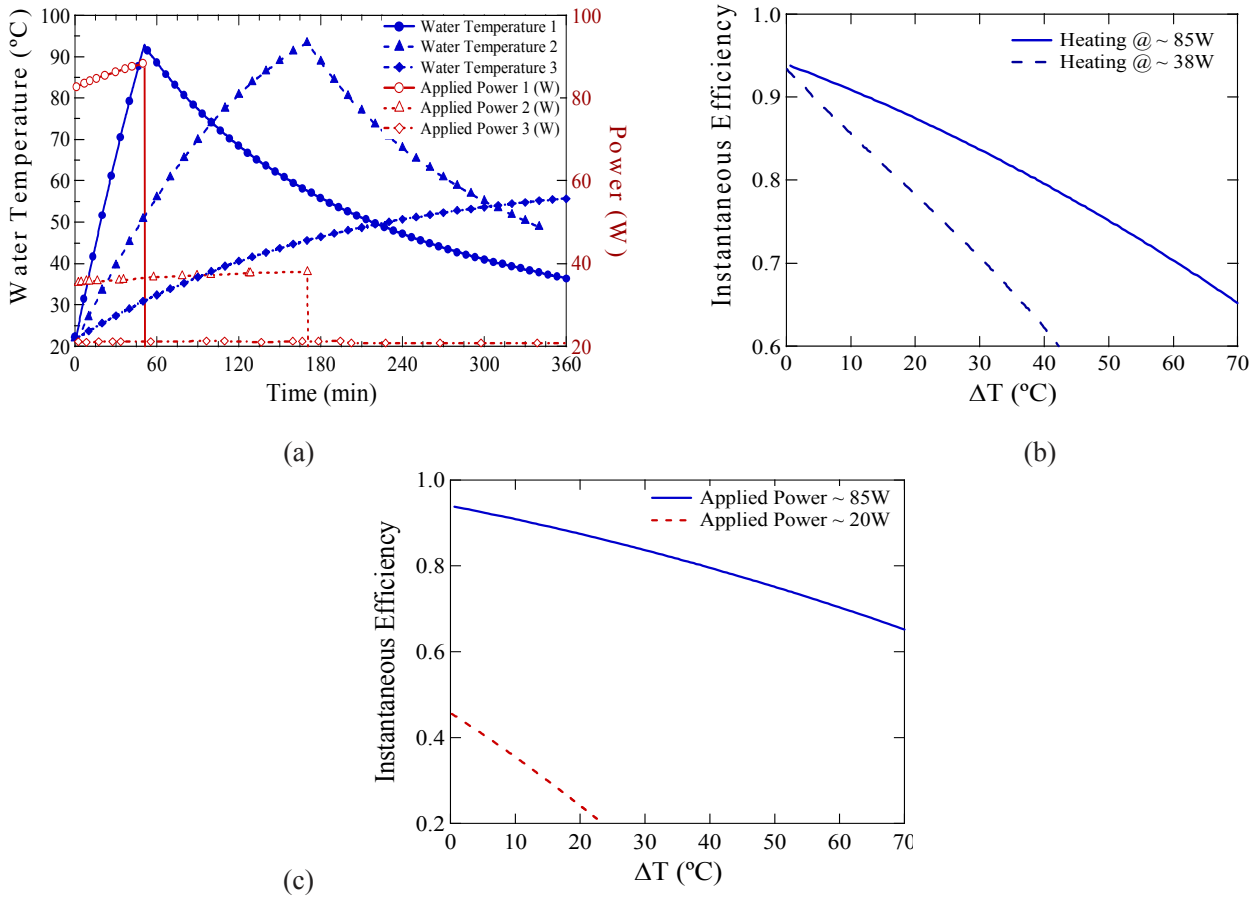

Fig. 7. Demonstration of Joule heating capabilities of the carbon nanotube-based solar selective coating: (a) Plot of temperature of 700 ml of water inside the ETC as current is applied to the coating to heat the water; (b) Calculated plot of instantaneous and cumulative efficiencies for water heating by Joule heating; (c) Plot of instantaneous efficiency versus the difference between water temperature and ambient.

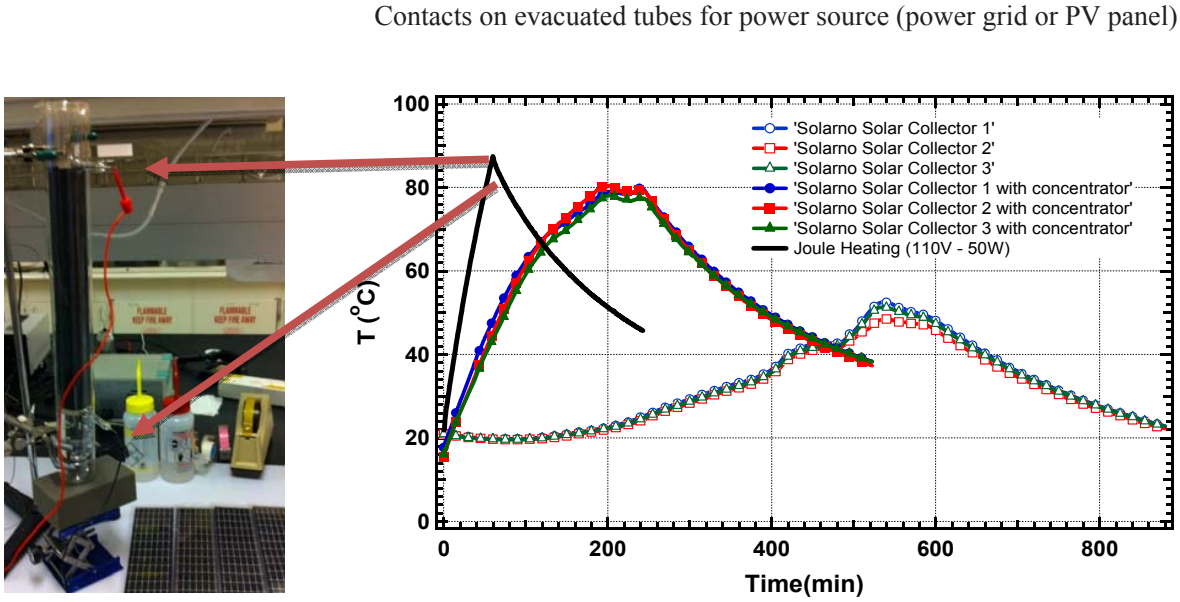

(a) (b)

Fig. 8. (a) Testing of evacuated tube with Joule heating. (b) Water temperature inside Solarno's CNT coated evacuated tube collectors.

The additional functionality of CNT coating that allows operation of SWH in the dark or while weather conditions are not favorable. The electric booster system is not part of all residential system is not required and the payback of system is further decreased. We propose to upscale prototype Joule heating evacuated tubes for commercial SWH systems. The tube fabricated for proof of concept is in length approximately a quarter of a commercial tube. The upscaling will require developing the CNT coating to maintain solar operation and also have the appropriate electrical properties for sufficient heating. The of CNT coating depend on thickness of coating (number of layers laminated). In the future one can develop coatings that will be directly compatible with the power grid. We also investigated the incorporation of PV panels at solar collector frame to supply the power.

4. Conclusions

Carbon nanotubes that can be dry spun from vertically oriented forests are an ideal material for lamination as solar selective coatings. We have shown that the dry lamination of CNT sheets allows the addition of any nanoparticles by any convenient method, such as spraying oxide nanoparticles for suppression of IR emission.

We have found an unexpected effect of emissivity decrease with densification of CNT sheets. There are two major advantages of using CNT laminated sheets as solar selective coatings in ETC: first of all Joule heating of the ETC is possible by conducting electric current through conductive CNT coatings, and as a second advantage we have extremely high thermal stability of CNT coatings, which allows to use ETC with CNT for concentrated sun industrial applications. Current limitations of CNT sheets based solar coatings is in still high IR emissivity at higher temperatures, which can be further eliminated by proper choice of an oxide or other nanoparticulate component for better selectivity, as is targeted in ongoing work.

Acknowledgements

We would like to acknowledge the financial support of this research in part by Welch Foundation grant 16-17 and CONACYT for academic opportunities and academic support. We also appreciate the partial support of the Ministry of Education and Science of the Russian Federation in the framework of Increase Competitiveness Program of NUST «MISiS» (№K2-2015-014). The partial support of PARASAT agency of Kazakhstan for development of advanced solar water heaters is highly appreciated.

References

[1]. International Energy Agency IEA. Solar Energy Perspectives. Solar Energy Perspectives (2011). doi:10.1787/9789264124585-en

[2]. International Energy Agency, I. Key World Energy Statistics 2016.

[3]. Christopher J. Koroneos, Evanthia A. Nanaki, J. Clean. Prod. 37 (2012) 154–161.
[4]. Y. Taheri, K. Alimardani, B.M.S. Ziapour, Heat Mass Transf. 51 (2015) 1403–1411.
[5]. R. Singh, I.J. Lazarus, M. Souliotis, Renew. Sustain. Energy Rev. 54 (2016) 270–298.
[6]. Y. Tian, C.Y. Zhao, Appl. Energy 104 (2013) 538–553.
[7]. N. Selvakumar, H.C. Barshilia, Sol. Energy Mater. Sol. Cells 98 (2012) 1–23.
[8]. H. Benli, Renew. Sustain. Energy Rev. 54 (2016) 99–109.
[9]. S.A. Kalogirou, S. Karellas, K. Braimakis, C. Stanciu, V. Badescu, Prog. Energy Combust. Sci. 56 (2016) 106–137.
[10]. S. Jaisankar, J. Ananth, S. Thulasi, S.T. Jayasuthakar, K.N. Sheeba, Renew. Sustain. Energy Rev. 15 (2011) 3045–3050.
[11]. S.A. Kalogirou, Prog. Energy Combust. Sci. 30 (2004) 231–295.
[12]. G.L. Morrison, I. Budihardjo, M. Behnia, Sol. Energy 76 (2004) 135–140.
[13]. C.C. Smith, & T.A. Weiss, Design application of the Hottel-Whillier-Bliss equation.
[14]. Z. Pluta, Journal of Power Technologies 91 (3) (2011) 158–164.
[15]. M.J. Ahmad, G.N. Tiwari, Open Renew. Energy J. 2 (2009) 19–24.
[16]. S. Limpa, Incidence angle modifiers: a general approach for energy calculations. 0–4
[17]. V. Dabra, L. Yadav, A. Yadav, Int. J. Eng. Sci. Technol. 5 (2013) 100–110.
[18]. Z.-P. Yang, L. Ci, J.A. Bur, S.-Y. Lin, & P.M. Ajayan, Experimental Observation of an Extremely Dark Material Made By a Low-Density Nanotube Array. doi:10.1021/nl072369t
[19]. Z. Chen, T. Boström, Sol. Energy Mater. Sol. Cells 144 (2016) 678–683.
[20]. E. Zambolin, D. Del. Col, Sol. Energy 84 (2010) 1382–1396.
[21]. Zhang, Mei, Shaoli Fang, Anvar A. Zakhidov, Sergey B. Lee, Ali E. Aliev, Christopher D. Williams, Ken R. Atkinson, and Ray H. Baughman. Science 309 (5738) (2005) 1215-1219.
[22]. C.P. Huynh, S.C. Hawkins Carbon 48 (2010) 1105–1115.
[23]. Ali E. Aliev, Csaba Guthy, Mei Zhang, Shaoli Fang, Anvar A. Zakhidov, John E. Fischer, Ray H. Baughman, Carbon 45 (2007) 2880–2888.
[24]. A.M. Marconnet, M.A. Panzer, K.E. Goodson, Thermal conduction phenomena in carbon nanotubes and related nanostructured materials. doi:10.1103/RevModPhys.85.1295
[25]. Wei Lin, Jintang Shang, Wentian Gu, C.P. Wong, Carbon 50 (2012) 1591–1603.
[26]. C.P. Huynh, S.C. Hawkins Carbon 48 (2010) 1105–1115.
[27]. Jaegeun Lee, Eugene Oh, Hye-Jin Kim, Seungho Cho, Teawon Kim, Sunghyun Lee, Junbeom Park, Hee Jin Kim, Kun-Hong Lee, J. Mater. Sci. 48 (2013) 6897–6904.
[28]. Ali E. Aliev, Csaba Guthy, Mei Zhang, Shaoli Fang, Anvar A. Zakhidov, John E. Fischer, Ray H. Baughman, Carbon 45 (15) (2007) 2880–2888
[29]. M.S. Dresselhaus, A. Jorio, A.G. Souza Filho, A.R. Saito, Trans. R. Soc. A 368 (2010) 5355–5377.
[30]. R.A. DiLeo, B.J. Landi, R.P. Raffaelle, J. Appl. Phys. 101 (2007) 64307–64311.